Orthogonal Time Frequency Space (OTFS) Modulation

Tutorial at VTC2018-Fall, Chicago, August 27th, 2018

A. Chockalingam,† **Yi Hong**‡**, Emanuele Viterbo**‡

† Department of Electrical and Communications Engineering
Indian Institute of Science, Bangalore, India

‡ Department of Electrical and Computer Systems Engineering
Monash University, Clayton, Australia

Special thanks to P.Raviteja, Khoa T.Phan, M.K.Ramachandran

Overview I

1. Introduction
   - Evolution of wireless
   - High-Doppler wireless channels
   - Conventional modulation schemes (e.g., OFDM)
   - Effect of high Dopplers in conventional modulation
2. Wireless channel representation
   - Time–frequency representation
   - Time–delay representation
   - Delay–Doppler representation
3. OTFS modulation
   - Signaling in the delay–Doppler domain
   - Roots in representation theory
   - OTFS signaling architecture
   - Compatibility with OFDM architecture

Overview II

4. OTFS signal detection
   - Vectorized formulation of the input-output relation
   - Message passing based detection
   - MCMC based detection
   - Performance results
5. OTFS channel estimation
   - PN-pilot based estimation for SISO-OTFS
   - Performance
6. MIMO/multiuser MIMO and precoding with OTFS
   - MIMO OTFS
   - Channel estimation in delay-Doppler domain
   - Multiuser OTFS

Link to download presentation slides:
https://ecse.monash.edu/staff/eviterbo/OTFS-VTC18/presentation_1.pdf
Link to download Matlab code:
https://ecse.monash.edu/staff/eviterbo/OTFS-VTC18/OTFS_sample_code.zip

Introduction

Evolution of wireless

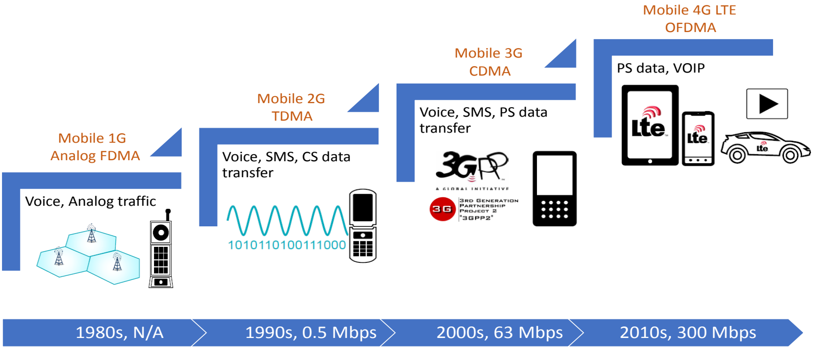

- Waveform design is the major change between the generations

High-Doppler wireless channels

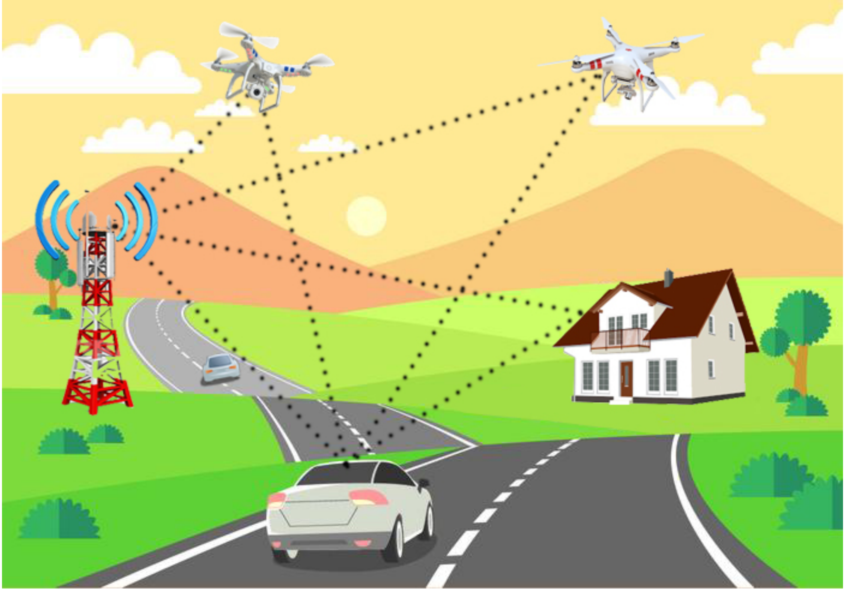

Wireless Channels - delay spread

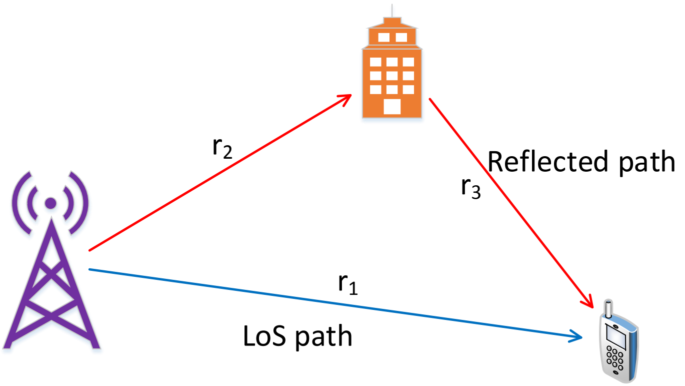

- Delay of LoS path: $\tau_1 = r_1/c$
- Delay of reflected path: $\tau_2 = (r_2 + r_3)/c$
- Delay spread: $\tau_2 - \tau_1$

Wirless Channels - Doppler spread

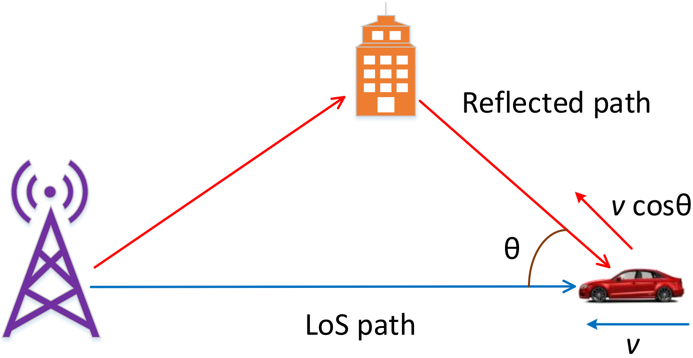

- Doppler frequency of LoS path: $\nu_1 = f_c \frac{v}{c}$
- Doppler frequency of reflected path: $\nu_2 = f_c \frac{v \cos\theta}{c}$
- Doppler spread: $\nu_2 - \nu_1$

Conventional modulation scheme – OFDM

- OFDM - Orthogonal Frequency Division Multiplexing

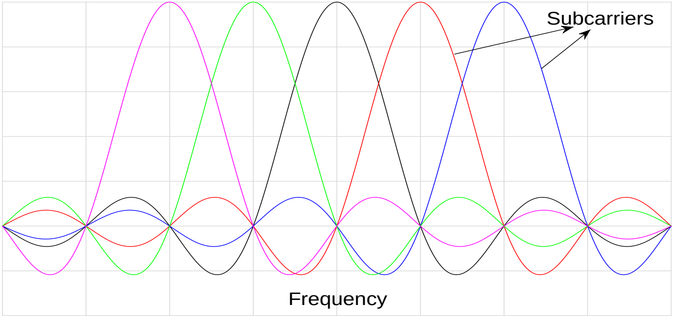

- OFDM divides the frequency selective channel into multiple parallel sub-channels

OFDM system model

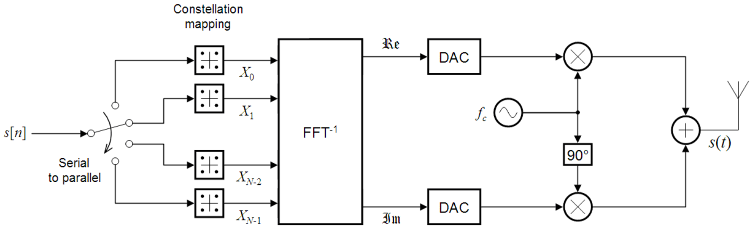

Figure: OFDM Tx

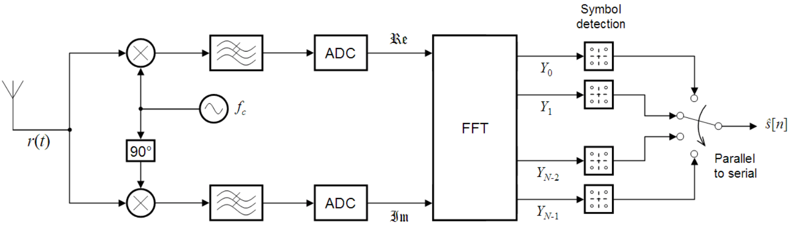

Figure: OFDM Rx

(*) From Wikipedia, the free encyclopedia

OFDM system model

- Received signal – channel is constant over OFDM symbol (no Doppler)
  $h_0, h_1, \cdots, h_{P-1}$ – Path gains over P multipaths

$$\mathbf{r} = \underbrace{\begin{bmatrix} h_0 & 0 & \cdots & 0 & h_{P-1} & h_{P-2} & \cdots & h_1 \\ h_1 & h_0 & \cdots & 0 & 0 & h_{P-1} & \cdots & h_2 \\ \vdots & \ddots & \ddots & \ddots & \ddots & \ddots & \ddots & \vdots \\ 0 & 0 & \cdots & h_{P-1} & h_{P-2} & \cdots & h_1 & h_0 \end{bmatrix}}_{\text{Circulant matrix } (\mathbf{H})} \mathbf{s}$$

$$= \sum_{i=0}^{P-1} h_i \mathbf{\Pi}^i \mathbf{s}; \mathbf{\Pi} \text{ is the permutation matrix, } \begin{bmatrix} 0 & \cdots & 0 & 1 \\ 1 & \ddots & 0 & 0 \\ \vdots & \ddots & \ddots & \vdots \\ 0 & \cdots & 1 & 0 \end{bmatrix} \text{(notation used later)}$$

$$= \mathbf{F}^H \mathbf{D} \mathbf{F} \mathbf{s}$$

$$\mathbf{y} = \mathbf{F}\mathbf{r} = \underbrace{\mathbf{D}}_{\text{Diagonal matrix}} \mathbf{x}$$

- OFDM Pros
  - Simple detection (one tap equalizer)
  - Efficiently combat the multi-path effects

Effect of high multiple Dopplers in OFDM

- **H** matrix lost the circulant structure – decomposition becomes erroneous
- Introduces inter carrier interference (ICI)

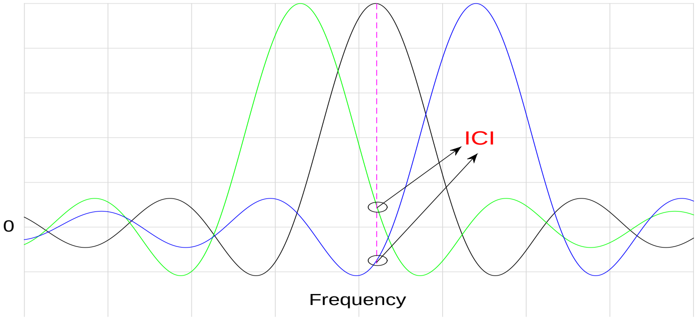

- OFDM Cons
  - multiple Dopplers are difficult to equalize
  - Sub-channel gains are not equal and lowest gain decides the performance

Effect of high Dopplers in OFDM

- Orthogonal Time Frequency Space Modulation (OTFS)(*)
  - Solves the two cons of OFDM
  - Works in Delay–Doppler domain rather than Time–Frequency domain

(*) R. Hadani, S. Rakib, M. Tsatsanis, A. Monk, A. J. Goldsmith, A. F. Molisch, and R. Calderbank, "Orthogonal time frequency space modulation," in *Proc. IEEE WCNC*, San Francisco, CA, USA, March 2017.

Wireless channel representation

- Different representations of linear time variant (LTV) wireless channels

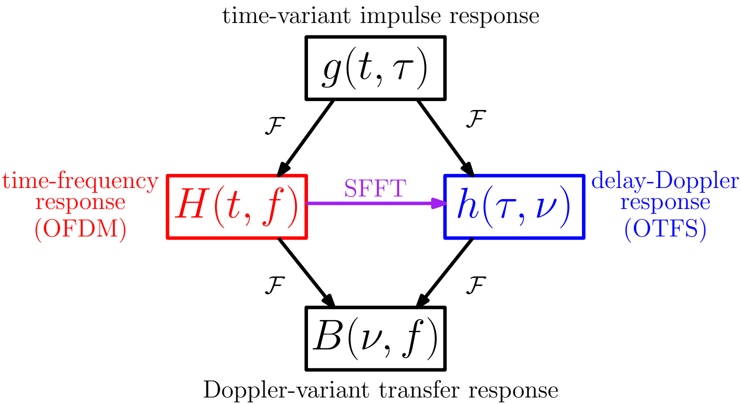

Wireless channel representation

- The received signal in linear time variant channel (LTV)

$$r(t) = \int \underbrace{g(t,\tau)}_{\text{time-variant impulse response}} s(t-\tau)d\tau \rightarrow \text{generalization of LTI}$$

$$= \int\int \underbrace{h(\tau,\nu)}_{\text{Delay–Doppler spreading function}} s(t-\tau)e^{j2\pi\nu t}d\tau d\nu \rightarrow \text{Delay–Doppler Channel}$$

$$= \int \underbrace{H(t,f)}_{\text{time-frequency response}} S(f)e^{j2\pi ft}df \rightarrow \text{Time–Frequency Channel}$$

- Relation between $h(\tau,\nu)$ and $H(t,f)$

$$\left.\begin{aligned} h(\tau,\nu) &= \int\int H(t,f)e^{-j2\pi(\nu t - f\tau)}dtdf \\ H(t,f) &= \int\int h(\tau,\nu)e^{j2\pi(\nu t - f\tau)}d\tau d\nu \end{aligned}\right\}\text{Pair of 2D symplectic FT}$$

Wireless channel representation

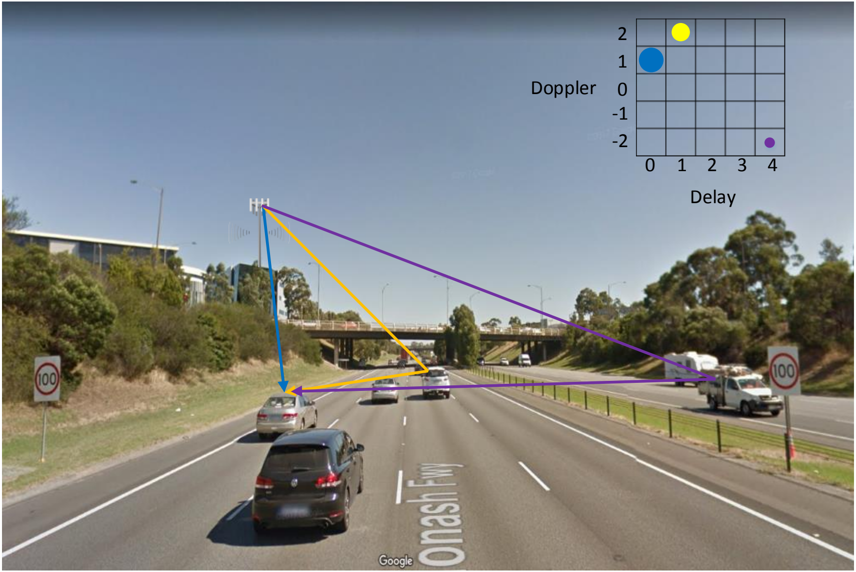

Wireless channel representation

Time-variant impulse response $g(t, \tau)$

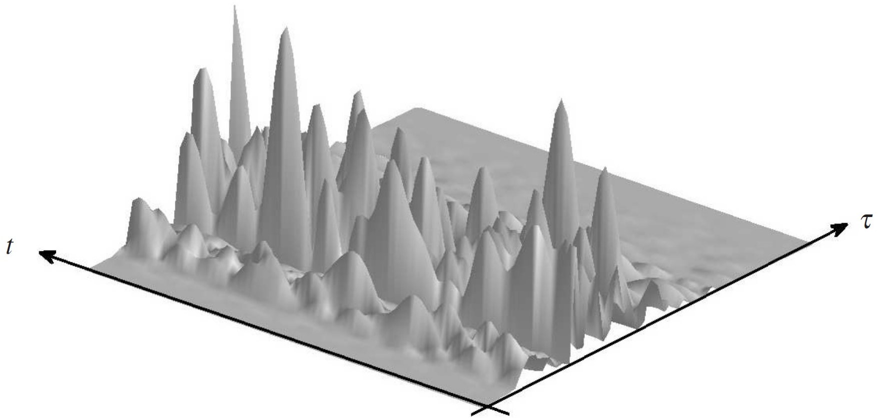

* G. Matz and F. Hlawatsch, *Chapter 1, Wireless Communications Over Rapidly Time-Varying Channels.* New York, NY, USA: Academic, 2011

Time-frequency and delay-Doppler responses

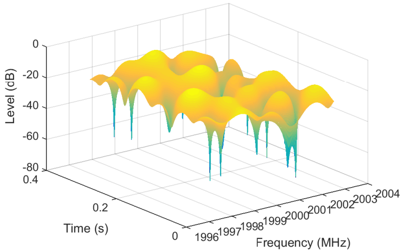

$\xrightarrow{\text{SFFT}}$

$\xleftarrow[\text{ISFFT}]{}$

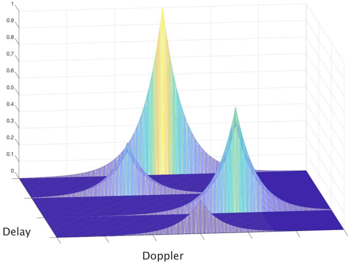

Channel in Time–frequency $H(t, f)$ and delay–Doppler $h(\tau, \nu)$

Time–Frequency and delay–Doppler grids

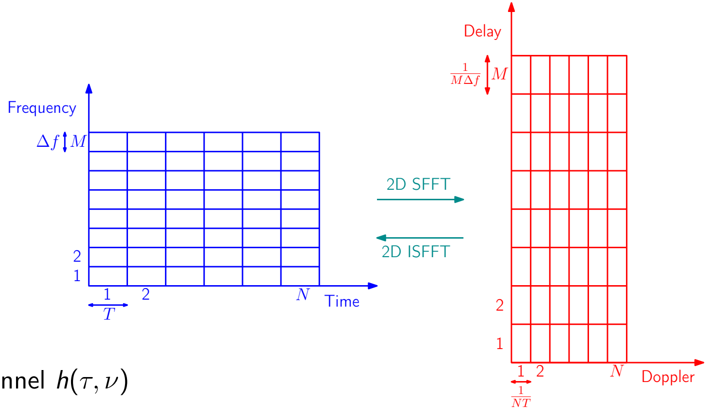

- Channel $h(\tau, \nu)$

$$h(\tau, \nu) = \sum_{i=1}^{P} h_i \delta(\tau - \tau_i)\delta(\nu - \nu_i)$$

- Assume $\tau_i = l_{\tau_i}\left(\frac{1}{M\Delta f}\right)$ and $\nu_i = k_{\nu_i}\left(\frac{1}{NT}\right)$

OTFS Parameters

Subcarrier spacing (Δf)	M	Bandwidth ($W = M\Delta f$)	Symbol duration ($T_s = 1/W$)	delay spread	$l_{\tau_{\max}}$
15 KHz	1024	**15 MHz**	0.067 μs	4.7 μs	71 ($\approx$ 7%)

Carrier frequency (f_c)	N	Latency ($NMT_s = NT$)	Doppler resolution ($1/NT$)	UE speed (v)	Doppler frequency ($f_d = f_c \frac{v}{c}$)	$k_{\nu_{\max}}$
4 GHz	128	**8.75 ms**	114 Hz	30 Kmph	111 Hz	1 ($\approx$ 1.5%)
				120 Kmph	444 Hz	4 ($\approx$ 6%)
				500 Kmph	1850 Hz	16($\approx$ 25%)

OTFS modulation

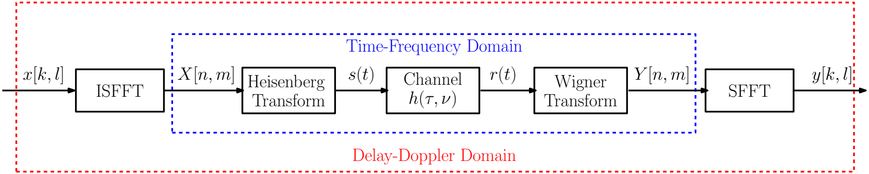

Figure: OTFS mod/demod

- Time–frequency domain is similar to an OFDM system with N symbols in a frame (Pulse-Shaped OFDM)

Time–frequency domain

- Modulator – Heisenberg transform

$$s(t) = \sum_{n=0}^{N-1} \sum_{m=0}^{M-1} X[n, m] g_{\text{tx}}(t - nT) e^{j2\pi m\Delta f(t-nT)}$$

- Simplifies to IFFT in the case of $N = 1$ and rectangular g_{tx}
- Channel

$$r(t) = \int H(t, f) S(f) e^{j2\pi ft} df$$

- Matched filter – Wigner transform

$$Y(t, f) = A_{g_{\text{rx}},r}(t, f) \triangleq \int g^*_{\text{rx}}(t' - t) r(t') e^{-j2\pi f(t'-t)} dt'$$

$$Y[n, m] = Y(t, f)|_{t=nT, f=m\Delta f}$$

- Simplifies to FFT in the case of $N = 1$ and rectangular g_{rx}

Time–frequency domain – ideal pulses

- If g_{tx} and g_{rx} are perfectly localized in time and frequency then they satisfy the bi-orthogonality condition and

$$Y[n,m] = H[n,m]X[n,m]$$

where

$$H[n,m] = \int\int h(\tau,\nu)e^{j2\pi\nu nT}e^{-j2\pi m\Delta f\tau}d\tau d\nu$$

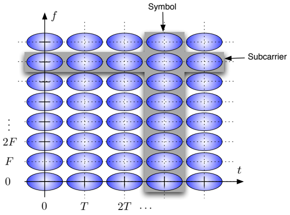

Figure: Time–frequency domain

* F. Hlawatsch and G. Matz, Eds., *Chapter 2, Wireless Communications Over Rapidly Time-Varying Channels.* New York, NY, USA: Academic, 2011 (PS-OFDM)

Signaling in the delay–Doppler domain

- Time–frequency input-output relation

$$Y[n,m] = H[n,m]X[n,m]$$

where

$$H[n,m] = \sum_{k}\sum_{l} h[k,l]\, e^{j2\pi\left(\frac{nk}{N}-\frac{ml}{M}\right)}$$

- ISFFT

$$X[n,m] = \frac{1}{\sqrt{NM}}\sum_{k=0}^{N-1}\sum_{l=0}^{M-1} x[k,l]e^{j2\pi\left(\frac{nk}{N}-\frac{ml}{M}\right)}$$

- SFFT

$$y[k,l] = \frac{1}{\sqrt{NM}}\sum_{n=0}^{N-1}\sum_{m=0}^{M-1} Y[n,m]e^{-j2\pi\left(\frac{nk}{N}-\frac{ml}{M}\right)}$$

Delay–Doppler domain input-output relation

- Received signal in delay–Doppler domain

$$y[k,l] = \sum_{i=1}^{P} h_i x[[k - k_{\nu_i}]_N, [l - l_{\tau_i}]_M]$$

$$= h[k,l] \circledast x[k,l] \qquad \text{(2D Circular Convolution)}$$

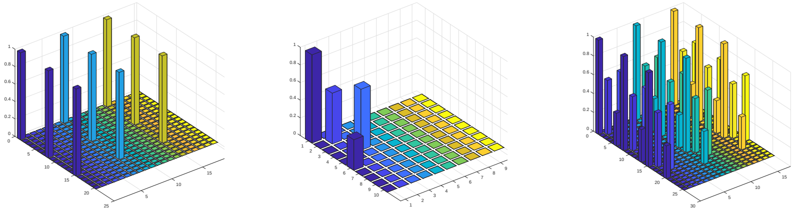

(a) Input signal, $x[k,l]$ (b) Channel, $h[k,l]$ (c) Output signal, $y[k,l]$

Figure: OTFS signals

Fractional doppler effect

- Actual Doppler may not be perfectly aligned with the grid

$$\nu_i = (k_{\nu_i} + \kappa_{\nu_i}) \left(\frac{1}{NT} \right), k_{\nu_i} \in \mathbb{Z}, -1/2 < \kappa_{\nu_i} < 1/2$$

- Induces interference from the neighbor points of k_{ν_i} in the Doppler grid due to non-orthogonality in channel relation – Inter Doppler Interference (IDI)
- Received signal equation becomes

$$y(k,l) = \sum_{i=1}^{P} \sum_{q=-N_i}^{N_i} h_i \left(\frac{e^{j2\pi(-q-\kappa_{\nu_i})} - 1}{Ne^{j\frac{2\pi}{N}(-q-\kappa_{\nu_i})} - N} \right) x\left[[k - k_{\nu_i} + q]_N, [l - l_{\tau_i}]_M\right]$$

Compatibility with OFDM architecture

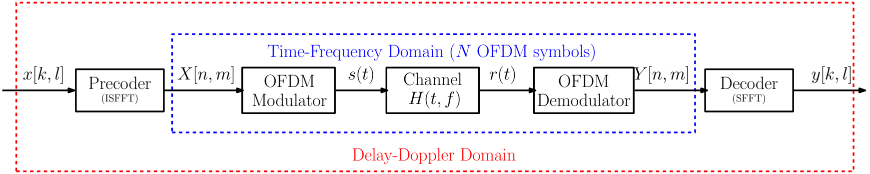

Figure: OTFS mod/demod

- OTFS is compatible with LTE system
- OTFS can be easily implemented by applying a precoding and decoding blocks on N consecutive OFDM symbols

OTFS with rectangular pulses – time–frequency domain

- Assume g_{tx} and g_{rx} to be rectangular pulses (same as OFDM) – don't follow bi-orthogonality condition
- Time–frequency input-output relation

$$Y[n,m] = H[n,m]X[n,m] + \text{ICI} + \text{ISI}$$

- ICI – loss of orthogonality in frequency domain due to Dopplers
- ISI – loss of orthogonality in time domain due to delays

(*) P. Raviteja, K. T. Phan, Y. Hong, and E. Viterbo, "Interference cancellation and iterative detection for orthogonal time frequency space modulation", accepted for publication *in IEEE Trans. Wireless Commun.*, July 2018. Available on: https://arxiv.org/abs/1802.05242 (Feb. 14, 2018)

OTFS: matrix representation

- Transmit signal at time–frequency domain: ISFFT+Heisenberg+pulse shaping on delay–Doppler

$$\mathbf{S} = \mathbf{G}_{\mathrm{tx}}\mathbf{F}_M^H \underbrace{(\mathbf{F}_M \mathbf{X} \mathbf{F}_N^H)}_{\text{ISFFT}} = \mathbf{G}_{\mathrm{tx}}\mathbf{X}\mathbf{F}_N^H$$

- In vector form:

$$\mathbf{s} = \mathrm{vec}(\mathbf{S}) = (\mathbf{F}_N^H \otimes \mathbf{G}_{\mathrm{tx}})\mathbf{x}$$

- Received signal at delay–Doppler domain: pulse shaping+Wigner+SFFT on time–frequency received signal

$$\mathbf{Y} = \mathbf{F}_M^H(\mathbf{F}_M \mathbf{G}_{\mathrm{rx}}\mathbf{R})\mathbf{F}_N$$

- In vector form:

$$\mathbf{y} = (\mathbf{F}_N \otimes \mathbf{G}_{\mathrm{rx}})\mathbf{r}$$

OTFS: matrix representation – channel

- Received signal in the time–frequency domain

$$r(t) = \int\int h(\tau,\nu)s(t-\tau)e^{j2\pi\nu(t-\tau)}d\tau d\nu + w(t)$$

- Channel

$$h(\tau,\nu) = \sum_{i=1}^{P} h_i \delta(\tau-\tau_i)\delta(\nu-\nu_i)$$

- Received signal in discrete form

$$r(n) = \sum_{i=1}^{P} h_i \underbrace{e^{\frac{j2\pi k_i(n-l_i)}{MN}}}_{\text{Doppler}} \underbrace{s([n-l_i]_{MN})}_{\text{Delay}} + w(n), 0 \le n \le MN-1$$

- Received signal in vector form

$$\mathbf{r} = \mathbf{H}\mathbf{s} + \mathbf{w}$$

- $\mathbf{H}$ is an $MN \times MN$ matrix of the following form

$$\mathbf{H} = \sum_{i=1}^{P} h_i \mathbf{\Pi}^{l_i} \mathbf{\Delta}^{(k_i)},$$

where, $\mathbf{\Pi}$ is the permutation matrix (forward cyclic shift), and $\mathbf{\Delta}^{(k_i)}$ is the diagonal matrix

$$\underbrace{\mathbf{\Pi} = \begin{bmatrix} 0 & \cdots & 0 & 1 \\ 1 & \ddots & 0 & 0 \\ \vdots & \ddots & \ddots & \vdots \\ 0 & \cdots & 1 & 0 \end{bmatrix}_{MN \times MN}}_{\text{Delay (similar to OFDM)}}, \quad \mathbf{\Delta}^{(k_i)} = \underbrace{\begin{bmatrix} e^{\frac{j2\pi k_i(0)}{MN}} & 0 & \cdots & 0 \\ 0 & e^{\frac{j2\pi k_i(1)}{MN}} & \cdots & 0 \\ \vdots & & \ddots & \vdots \\ 0 & 0 & \cdots & e^{\frac{j2\pi k_i(MN-1)}{MN}} \end{bmatrix}}_{\text{Doppler}}$$

OTFS: matrix representation – channel

- Received signal at delay–Doppler domain

$$\begin{aligned}\mathbf{y} &= \left[(\mathbf{F}_N \otimes \mathbf{G}_{\mathrm{rx}})\mathbf{H}(\mathbf{F}_N^H \otimes \mathbf{G}_{\mathrm{tx}})\right]\mathbf{x} + (\mathbf{F}_N \otimes \mathbf{G}_{\mathrm{rx}})\mathbf{w} \\ &= \mathbf{H}_{\mathrm{eff}}\mathbf{x} + \widetilde{\mathbf{w}}\end{aligned}$$

- Effective channel for arbitrary pulses

$$\begin{aligned}\mathbf{H}_{\mathrm{eff}} &= (\mathbf{I}_N \otimes \mathbf{G}_{\mathrm{rx}})(\mathbf{F}_N \otimes \mathbf{I}_M)\mathbf{H}(\mathbf{F}_N^H \otimes \mathbf{I}_M)(\mathbf{I}_N \otimes \mathbf{G}_{\mathrm{tx}}) \\ &= (\mathbf{I}_N \otimes \mathbf{G}_{\mathrm{rx}})\underbrace{\mathbf{H}_{\mathrm{eff}}^{\mathrm{rect}}}_{\text{Channel for rectangular pulses } (\mathbf{G}_{\mathrm{tx}}=\mathbf{G}_{\mathrm{rx}}=\mathbf{I}_M)}(\mathbf{I}_N \otimes \mathbf{G}_{\mathrm{tx}})\end{aligned}$$

- Effective channel for rectangular pulses

$$\mathbf{H}_{\mathrm{eff}}^{\mathrm{rect}} = \sum_{i=1}^{P} h_i \underbrace{\left[(\mathbf{F}_N \otimes \mathbf{I}_M)\mathbf{\Pi}^{l_i}(\mathbf{F}_N^H \otimes \mathbf{I}_M)\right]}_{\mathbf{P}^{(i)} \text{ (delay)}} \underbrace{\left[(\mathbf{F}_N \otimes \mathbf{I}_M)\mathbf{\Delta}^{(k_i)}(\mathbf{F}_N^H \otimes \mathbf{I}_M)\right]}_{\mathbf{Q}^{(i)} \text{ (Doppler)}}$$

$$= \sum_{i=1}^{P} h_i \mathbf{P}^{(i)}\mathbf{Q}^{(i)} = \sum_{i=1}^{P} h_i \mathbf{T}^{(i)}$$

OTFS: Example for computing $\mathbf{H}_{\text{eff}}^{\text{rect}}$

- $M = 2,\ N = 2, MN = 4$
- $l_i = 0$ and $k_i = 0$ (no delay and Doppler)
  - $\mathbf{\Pi}^{l_i=0} = \mathbf{I}_4 \Rightarrow \mathbf{P}^{(i)} = (\mathbf{F}_2 \otimes \mathbf{I}_2)(\mathbf{F}_2^H \otimes \mathbf{I}_2) = \mathbf{I}_4$
  - $\mathbf{\Delta}^{(k_i=0)} = \mathbf{I}_4 \Rightarrow \mathbf{Q}^{(i)} = (\mathbf{F}_2 \otimes \mathbf{I}_2)(\mathbf{F}_2^H \otimes \mathbf{I}_2) = \mathbf{I}_4$
  - $\mathbf{T}^{(i)} = \mathbf{P}^{(i)}\mathbf{Q}^{(i)} = \mathbf{I}_4 \Rightarrow$ Narrowband channel

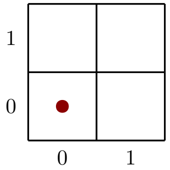

OTFS: Example for computing $\mathbf{H}_{\text{eff}}^{\text{rect}}$

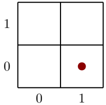

- $l_i = 1$ and $k_i = 0$ (delay but no Doppler)
  - $\mathbf{\Pi}^{l_i=1} = \begin{bmatrix} 0 & 0 & 0 & 1 \\ 1 & 0 & 0 & 0 \\ 0 & 1 & 0 & 0 \\ 0 & 0 & 1 & 0 \end{bmatrix} \Rightarrow$ block circulant matrix with 2×2 $(M \times M)$ block size
  - $\mathbf{P}^{(i)} = (\mathbf{F}_2 \otimes \mathbf{I}_2)\mathbf{\Pi}(\mathbf{F}_2^H \otimes \mathbf{I}_2) = \begin{bmatrix} 0 & 1 & 0 & 0 \\ 1 & 0 & 0 & 0 \\ 0 & 0 & 0 & e^{-j2\pi\frac{1}{2}} \\ 0 & 0 & 1 & 0 \end{bmatrix}$

    (using the block circulant matrix decomposition $\rightarrow$ generalization of circulant matrix decomposition in OFDM)
  - $\mathbf{\Delta}^{(k_i=0)} = \mathbf{I}_4 \Rightarrow \mathbf{Q}^{(i)} = (\mathbf{F}_2 \otimes \mathbf{I}_2)(\mathbf{F}_2^H \otimes \mathbf{I}_2) = \mathbf{I}_4$
  - $\mathbf{T}^{(i)} = \mathbf{P}^{(i)} \Rightarrow \mathbf{T}^{(i)}\mathbf{s} \rightarrow$ circularly shifts the elements in each block (size M) of $\mathbf{s}$ by 1 (delay shift)

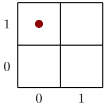

- $l_i = 0$ and $k_i = 1$ (Doppler but no delay)
  - $\mathbf{\Pi}^{l_i=0} = \mathbf{I}_4 \Rightarrow \mathbf{P}^{(i)} = (\mathbf{F}_2 \otimes \mathbf{I}_2)(\mathbf{F}_2^H \otimes \mathbf{I}_2) = \mathbf{I}_4$
  - $\mathbf{\Delta}^{(k_i=1)} = \begin{bmatrix} 1 & 0 & 0 & 0 \\ 0 & e^{j2\pi\frac{1}{4}} & 0 & 0 \\ 0 & 0 & e^{j2\pi\frac{2}{4}} & 0 \\ 0 & 0 & 0 & e^{j2\pi\frac{3}{4}} \end{bmatrix} \Rightarrow$ block diagonal matrix with 2×2 ($M \times M$) block size
  - $\mathbf{Q}^{(i)} = (\mathbf{F}_2 \otimes \mathbf{I}_2)\mathbf{\Delta}^{(1)}(\mathbf{F}_2^H \otimes \mathbf{I}_2) = \begin{bmatrix} 0 & 0 & 1 & 0 \\ 0 & 0 & 0 & e^{j2\pi\frac{1}{4}} \\ 1 & 0 & 0 & 0 \\ 0 & e^{j2\pi\frac{1}{4}} & 0 & 0 \end{bmatrix}$
    (using the block circulant matrix decomposition in reverse direction)
  - $\mathbf{T}^{(i)} = \mathbf{Q}^{(i)} \Rightarrow \mathbf{T}^{(i)}\mathbf{s} \rightarrow$ circularly shifts the blocks (size M) of $\mathbf{s}$ by 1 (Doppler shift)

OTFS: Example for computing $\mathbf{H}_{\text{eff}}^{\text{rect}}$

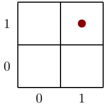

- $l_i = 1$ and $k_i = 1$ (both delay and Doppler)
  - $\mathbf{P}^{(i)} = \begin{bmatrix} 0 & 1 & 0 & 0 \\ 1 & 0 & 0 & 0 \\ 0 & 0 & 0 & e^{-j2\pi\frac{1}{2}} \\ 0 & 0 & 1 & 0 \end{bmatrix}$
  - $\mathbf{Q}^{(i)} = \begin{bmatrix} 0 & 0 & 1 & 0 \\ 0 & 0 & 0 & e^{j2\pi\frac{1}{4}} \\ 1 & 0 & 0 & 0 \\ 0 & e^{j2\pi\frac{1}{4}} & 0 & 0 \end{bmatrix}$
  - $\mathbf{T}^{(i)} = \mathbf{P}^{(i)}\mathbf{Q}^{(i)} \Rightarrow \mathbf{T}^{(i)}\mathbf{s} \rightarrow$ circularly shifts both the blocks (size M) and the elements in each block of $\mathbf{s}$ by 1 (delay and Doppler shifts)

OTFS: channel for rectangular pulses

- $\mathbf{T}^{(i)}$ has only one non-zero element in each row and the position and value of the non-zero element depends on the delay and Doppler values.

$$\mathbf{T}^{(i)}(p,q) = \begin{cases} e^{-j2\pi\frac{n}{N}} e^{j2\pi\frac{k_i([m-l_i]_M)}{MN}}, & \text{if } q = [m-l_i]_M + M[n-k_i]_N \text{ and } m < l_i \\ e^{j2\pi\frac{k_i([m-l_i]_M)}{MN}}, & \text{if } q = [m-l_i]_M + M[n-k_i]_N \text{ and } m \geq l_i \\ 0, & \text{otherwise.} \end{cases}$$

- Example: $l_i = 1$ and $k_i = 1$

$$\mathbf{T}^{(i)} = \begin{bmatrix} 0 & 0 & 0 & e^{j2\pi\frac{1}{4}} \\ 0 & 0 & 1 & 0 \\ 0 & e^{-j2\pi\frac{1}{4}} & 0 & 0 \\ 1 & 0 & 0 & 0 \end{bmatrix}$$

Vectorized formulation of the input-output relation

- The input-output relation in the delay–Doppler domain is a 2D convolution (with i.i.d. additive noise $w[k,l]$)

$$y[k,l] = \sum_{i=1}^{P} h_i x[[k - k_{\nu_i}]_N, [l - l_{\tau_i}]_M] + w[k,l] \quad k = 1 \dots N, l = 1 \dots M \qquad (1)$$

- Detection of information symbols $x[k,l]$ requires a deconvolution operation i.e., the solution of the linear system of NM equations

$$\mathbf{y} = \mathbf{H}\mathbf{x} + \mathbf{w} \qquad (2)$$

  where $\mathbf{x}, \mathbf{y}, \mathbf{w}$ are $x[k,l], y[k,l], w[k,l]$ in vectorized form and $\mathbf{H}$ is the $NM \times NM$ coefficient matrix of (1).

- Given the sparse nature of $\mathbf{H}$ we can solve (2) by using a message passing algorithm similar to (*)

(*) P. Som, T. Datta, N. Srinidhi, A. Chockalingam, and B. S. Rajan, "Low-complexity detection in large-dimension MIMO-ISI channels using graphical models," *IEEE J. Sel. Topics in Signal Processing*, vol. 5, no. 8, pp. 1497-1511, December 2011.

Message passing based detection

- Symbol-by-symbol MAP detection

$$
\begin{aligned}
\widehat{x}[c] &= \arg\max_{a_j \in \mathbb{A}} \Pr\left(x[c] = a_j \,\middle|\, \mathbf{y}, \mathbf{H}\right) \\
&= \arg\max_{a_j \in \mathbb{A}} \frac{1}{Q} \Pr\left(\mathbf{y} \,\middle|\, x[c] = a_j, \mathbf{H}\right) \\
&\approx \arg\max_{a_j \in \mathbb{A}} \prod_{d \in \mathcal{J}_c} \Pr\left(y[d] \,\middle|\, x[c] = a_j, \mathbf{H}\right)
\end{aligned}
$$

- Received signal $y[d]$

$$
y[d] = x[c]H[d,c] + \underbrace{\sum_{e \in \mathcal{I}(d), e \neq c} x[e]H[d,e] + z[d]}_{\zeta_{d,c}^{(i)} \rightarrow \text{ assumed to be Gaussian}}
$$

Messages in factor graph

Algorithm 1 MP algorithm for OTFS symbol detection

Input: Received signal $\mathbf{y}$, channel matrix $\mathbf{H}$

Initialization: pmf $\mathbf{p}_{c,d}^{(0)} = 1/Q$ **repeat**

- Observation nodes send the mean and variance to variable nodes
- Variable nodes send the pmf to the observation nodes
- Update the decision

until *Stopping criteria*;

Output: The decision on transmitted symbols $\widehat{x}[c]$

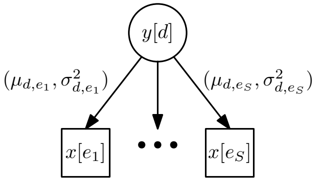

$\{e_1, e_2, \cdots, e_S\} = \mathcal{I}_d$

Observation node messages

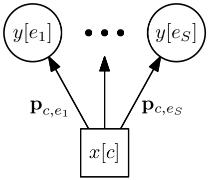

$\{e_1, e_2, \cdots, e_S\} = \mathcal{J}_c$

Variable node messages

Messages in factor graph – observation node messages

- Received signal

$$y[d] = x[c]H[d,c] + \underbrace{\sum_{e\in\mathcal{I}(d),e\neq c} x[e]H[d,e] + z[d]}_{\zeta_{d,c}^{(i)} \rightarrow \text{ assumed to be Gaussian}}$$

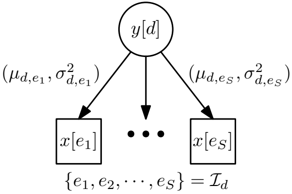

- Mean and Variance

$$\mu_{d,c}^{(i)} = \sum_{e\in\mathcal{I}(d),e\neq c} \sum_{j=1}^{Q} p_{e,d}^{(i-1)}(a_j) a_j H[d,e]$$

$$(\sigma_{d,c}^{(i)})^2 = \sum_{e\in\mathcal{I}(d),e\neq c} \left(\sum_{j=1}^{Q} p_{e,d}^{(i-1)}(a_j)|a_j|^2 |H[d,e]|^2 - \left| \sum_{j=1}^{Q} p_{e,d}^{(i-1)}(a_j) a_j H[d,e] \right|^2 \right) + \sigma^2$$

Messages in factor graph – variable node messages

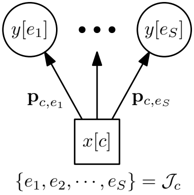

- Probability update with damping factor Δ

$$p_{c,d}^{(i)}(a_j) = \Delta \cdot \tilde{p}_{c,d}^{(i)}(a_j) + (1-\Delta) \cdot p_{c,d}^{(i-1)}(a_j), \, a_j \in \mathbb{A}$$

where

$$\tilde{p}_{c,d}^{(i)}(a_j) \propto \prod_{e \in \mathcal{J}(c), e \neq d} \Pr\left(y[e] \middle| x[c] = a_j, \mathbf{H}\right)$$

$$= \prod_{e \in \mathcal{J}(c), e \neq d} \frac{\xi^{(i)}(e,c,j)}{\sum_{k=1}^{Q} \xi^{(i)}(e,c,k)}$$

$$\xi^{(i)}(e,c,k) = \exp\left(\frac{-\left| y[e] - \mu_{e,c}^{(i)} - H_{e,c} a_k \right|^2}{(\sigma_{e,c}^{(i)})^2} \right)$$

Final update and stopping criterion

- Final update

$$p_c^{(i)}(a_j) = \prod_{e \in \mathcal{J}(c)} \frac{\xi^{(i)}(e,c,j)}{\sum_{k=1}^{Q} \xi^{(i)}(e,c,k)}$$

$$\widehat{x}[c] = \arg\max_{a_j \in \mathbb{A}} \; p_c^{(i)}(a_j), \quad c = 1, \cdots, NM.$$

- Stopping Criterion
  - Convergence Indicator $\eta^{(i)} = 1$

$$\eta^{(i)} = \frac{1}{NM} \sum_{c=1}^{NM} \mathbb{I}\left(\max_{a_j \in \mathbb{A}} \; p_c^{(i)}(a_j) \geq 0.99 \right)$$

  - Maximum number of Iterations
- Complexity (linear) – $\mathcal{O}(n_{iter}SQ)$ per symbol which is much less even compared to a linear MMSE detector $\mathcal{O}((NM)^2)$

Simulation results – damping factor Δ

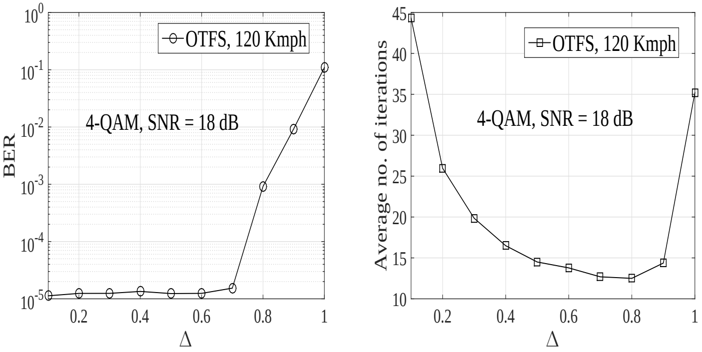

Figure: Variation of BER and average iterations no. with Δ. Optimal for $\Delta = 0.7$

Simulation results – OTFS vs OFDM with ideal pulses

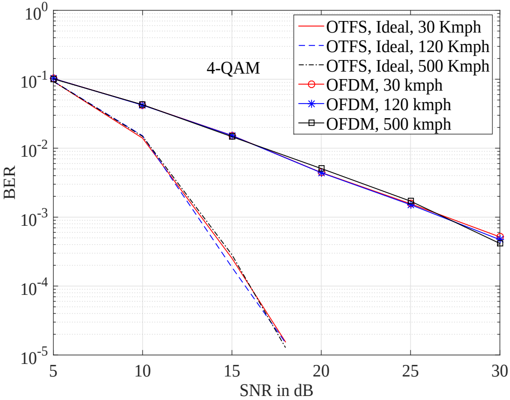

Figure: The BER performance comparison between OTFS with ideal pulses and OFDM systems at different Doppler frequencies.

Simulation results – IDI effect

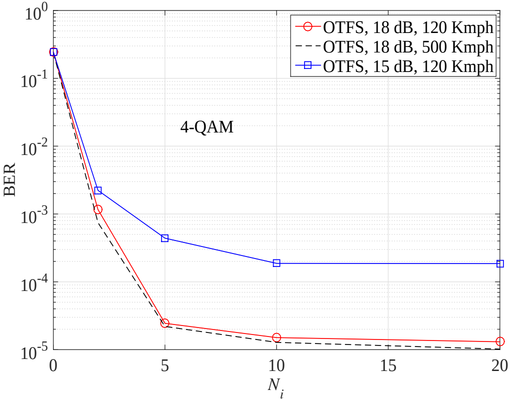

Figure: The BER performance of OTFS for different number of interference terms N_i with 4-QAM.

Simulation results – Ideal and Rectangular pulses

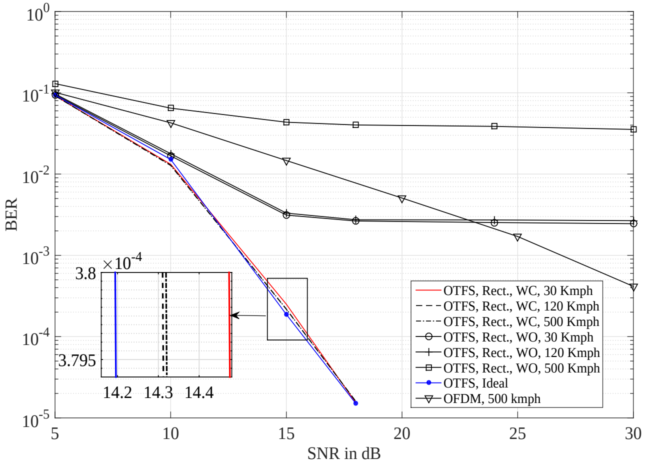

Figure: The BER performance of OTFS with rectangular and ideal pulses at different Doppler frequencies for 4-QAM.

Simulation results – Ideal and Rect. pulses - 16-QAM

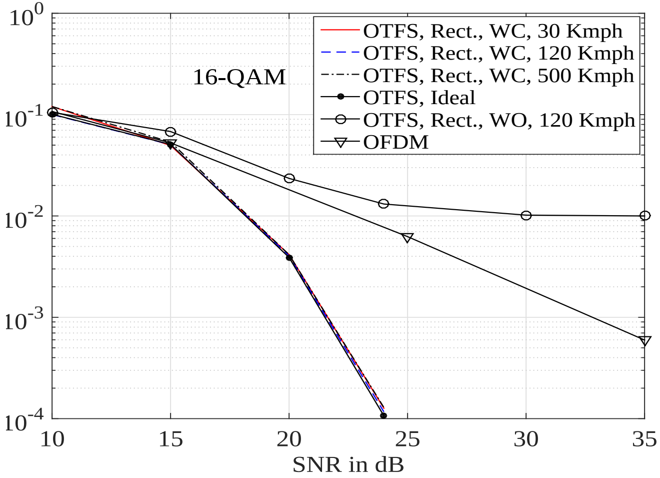

Figure: The BER performance of OTFS with rectangular and ideal pulses at different Doppler frequencies for 16-QAM.

Simulation results – Low latency

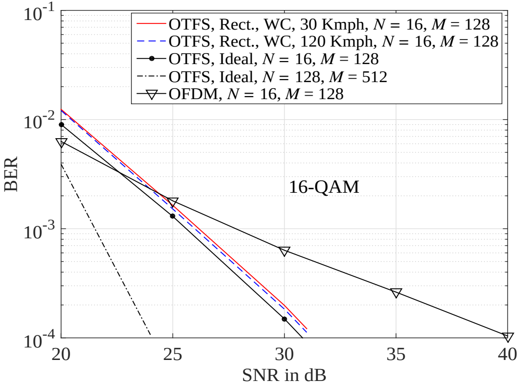

Figure: The BER performance of OTFS with rectangular pulses and low latency ($N = 16$, $T_f \approx 1.1$ ms).

Matlab code

- OTFS_sample_code.m

  → OTFS_modulation – 1. ISFFT, 2. Heisenberg transform

```
X = fft(ifft(x).').'/sqrt(M/N); % ISFFT
s_mat = ifft(X.')*sqrt(M); % Heisenberg transform
s = s_mat(:);
```

  → OTFS_channel_gen – generates wireless channel

  output: (delay_taps,Doppler_taps,chan_coef)

  → OTFS_channel_output – wireless channel and noise

```
L = max(delay_taps);
s = [s(N*M-L+1:N*M);s];% add one cp
s_chan = 0;
for itao = 1:taps
    s_chan = s_chan+chan_coef(itao)*circshift([s.*exp(1j*2*pi/M...
    *(-L:-L+length(s)-1)*Doppler_taps(itao)/N).';zeros(L,1)],delay_taps(itao));
end
noise = sqrt(sigma_2/2)*(randn(size(s_chan)) + 1i*randn(size(s_chan)));
r = s_chan + noise;
r = r(L+1:L+(N*M));% discard cp
```

Matlab code

→ OTFS_demodulation – 1. Wiegner transform, 2. SFFT

```
r_mat = reshape(r,M,N);
Y = fft(r_mat)/sqrt(M); % Wigner transform
Y = Y.';
y = ifft(fft(Y).').'/sqrt(N/M); % SFFT
```

→ OTFS_mp_detector – message passing detector

OTFS signal detection using MCMC sampling

- Maximum likelihood decision rule

$$\hat{\mathbf{x}}_{ML} = \arg\min_{\mathbf{x}\in\mathbb{A}^{NM}} ||\mathbf{y} - \mathbf{H}\mathbf{x}||^2$$

- Approximate solution using Gibbs sampling based MCMC technique
- Joint probability distribution for detection

$$p(x_1, x_2, \cdots, x_{NM}|\mathbf{y}, \mathbf{H}) \propto \exp\left(-\frac{||\mathbf{y} - \mathbf{H}\mathbf{x}||^2}{\sigma^2}\right)$$

Gibbs sampling

- All the NM coordinates are updated in every iteration by sampling from the following distributions (starting from a random initial vector)

$$
\begin{aligned}
x_1^{(t+1)} &\sim p\big(x_1|x_2^{(t)}, x_3^{(t)}, \cdots, x_{NM}^{(t)}, \mathbf{y}, \mathbf{H}\big) \\
x_2^{(t+1)} &\sim p\big(x_2|x_1^{(t+1)}, x_3^{(t)}, \cdots, x_{NM}^{(t)}, \mathbf{y}, \mathbf{H}\big) \\
x_3^{(t+1)} &\sim p\big(x_3|x_1^{(t+1)}, x_2^{(t+1)}, x_4^{(t)}, \cdots, x_{NM}^{(t)}, \mathbf{y}, \mathbf{H}\big) \\
&\vdots \\
x_{NM}^{(t+1)} &\sim p\big(x_{NM}|x_1^{(t+1)}, x_2^{(t+1)}, \cdots, x_{NM-1}^{(t+1)}, \mathbf{y}, \mathbf{H}\big)
\end{aligned}
$$

- Vector with the least ML cost $f_{ML} = ||\mathbf{y} - \mathbf{Hx}||^2$ in all iterations upto that iteration chosen as the detected vector

- Gibbs sampling with temperature parameter α

$$p(x_1, x_2, \cdots, x_{NM}|\mathbf{y}, \mathbf{H}) \propto \exp\left(-\frac{||\mathbf{y} - \mathbf{Hx}||^2}{\alpha^2\sigma^2} \right)$$

- Randomized Gibbs sampling based detection
  - Use a randomized rule with probability $r = \frac{1}{NM}$
  - Generate $|\mathbb{A}|$ probability values from a uniform distribution given by

$$p(x_i^{(t+1)} = i) \sim U[0, 1], \ \forall i \in \mathbb{A}$$

    such that $\sum_{i=1}^{|\mathbb{A}|} p(x_i^{(t+1)} = i) = 1$, and sample $x_k^{(t+1)}$ from this pdf
  - With probability $(1 - r)$, the conventional Gibbs sampling is used

---

(*) T. Datta, N. Ashok Kumar, A. Chockalingam, and B. Sundar Rajan, "A novel Monte-Carlo-sampling-based receiver for large-scale uplink multiuser MIMO systems," *IEEE Trans. Veh. Tech.*, vol. 62, no. 7, pp. 3019-3038, Sep. 2013.

Results and discussion

- Number of signal taps $P = 5$, parameter $N_i = 4$
- Doppler model: $\nu_i = \nu_{max} cos(\theta_i)$ where $\theta_i \sim \mathcal{U}(0, \pi)$
- Delay model:

Path index (i)	1	2	3	4	5
Excess Delay (τ_i)	$0\mu s$	$2.1\mu s$	$4.2\mu s$	$6.3\mu s$	$8.4\mu s$

- Simulation parameters

Parameter	**Value**
Carrier frequency (GHz)	4
Subcarrier spacing (kHz)	3.75
Frame size (M, N)	$(128, 32)$
Modulation scheme	BPSK
UE speed (kmph)	27, 120, 500
Channel estimation	Perfect

Table: Simulation parameters.

BER performance for 3 different Doppler values

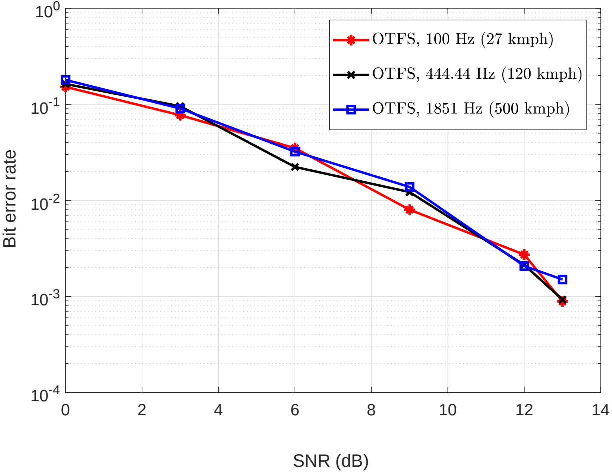

Figure: Randomized MCMC detection

Performance comparison with OFDM

- One frame consists of N consecutive OFDM blocks of size M and the transmit vector $\mathbf{x}_{\text{OFDM}} \in \mathbb{C}^{NM \times 1}$
- Consider the channel with P taps, $h(\tau, \nu) = \sum_{i=1}^{P} h_i \delta(\tau - \tau_i)\delta(\nu - \nu_i)$
- The time-delay representation is, $h(\tau, t) = \sum_{i=1}^{P} h_i e^{j2\pi\nu_i t} \delta(\tau - \tau_i)$
- Sample the time axis at $t = nTs$. The sampled time-delay representation, $h(\tau, n) = \sum_{i=1}^{P} h_i e^{\frac{j2\pi\nu_i n}{M\Delta f}} \delta(\tau - \tau_i)$
- Let $CP = P - 1$ denote the cyclic prefix length used and let $L = M + CP$. Size of one frame after cyclic prefix insertion to each block will then be NL.

Vectorized formulation of input-output relation

Notations:

- $\mathbf{T}_{CP} = [\mathbf{C}_{CP}^T \ \mathbf{I}_M]^T$ - $L \times M$ matrix that inserts cyclic prefix for one block, where $\mathbf{C}_{CP}$ contains the last CP rows of the identity matrix $\mathbf{I}_M$
- $\mathbf{R}_{CP} = [\mathbf{0}_{M \times CP} \ \mathbf{I}_M]$ - $M \times L$ matrix that removes the cyclic prefix for one block
- $\mathbf{W}_{M \times M}$ and $\mathbf{W}_{M \times M}^H$ - DFT and IDFT matrices of size M
- $\mathbf{B}_{cpin} = \text{diag}\underbrace{(\mathbf{T}_{CP}, \mathbf{T}_{CP}, \cdots, \mathbf{T}_{CP})}_{N \ times}$ - cyclic prefix insertion matrix for N consecutive OFDM blocks
- $\mathbf{B}_{cpre} = \text{diag}\underbrace{(\mathbf{R}_{CP}, \mathbf{R}_{CP}, \cdots, \mathbf{R}_{CP})}_{N \ times}$ - cyclic prefix removal matrix for N consecutive OFDM blocks

- $\mathbf{D} = \text{diag}\underbrace{(\mathbf{W}, \mathbf{W}, \cdots, \mathbf{W})}_{N\ \ times}$ - DFT matrix for N consecutive OFDM blocks
- $\mathbf{D}^H = \text{diag}\underbrace{(\mathbf{W}^H, \mathbf{W}^H, \cdots, \mathbf{W}^H)}_{N\ \ times}$ - IDFT matrix for N consecutive OFDM blocks
- The channel in the time-delay domain for a given frame can be written as a matrix $\mathbf{H}_{td}$ using $h(\tau, n) = \sum_{i=1}^{P} h_i e^{\frac{j2\pi\nu_i n}{M\Delta f}} \delta(\tau - \tau_i)$ and has size $NL \times NL$
- End-to-end relationship in OFDM modulation

$$\begin{aligned}\mathbf{y}_{\text{OFDM}} &= \underbrace{\mathbf{D}\mathbf{B}_{cpre}\mathbf{H}_{td}\mathbf{B}_{cpin}\mathbf{D}^H}_{\mathbf{H}_{\text{OFDM}}}\mathbf{x}_{\text{OFDM}} + \mathbf{v} \\ &= \mathbf{H}_{\text{OFDM}}\mathbf{x}_{\text{OFDM}} + \mathbf{v},\end{aligned}$$

where $\mathbf{x}_{\text{OFDM}}, \mathbf{y}_{\text{OFDM}}, \mathbf{v} \in \mathbb{C}^{NM\times 1}$, $\mathbf{H}_{\text{OFDM}} \in \mathbb{C}^{NM\times NM}$

BER performance comparison between OTFS and OFDM

- $\kappa_{\nu_i} = 0$ (no IDI) is assumed
- Delay and Doppler models

Path index (i)	1	2	3	4	5
Delay (τ_i,μs)	2.1	4.2	6.3	8.4	10.4
Doppler (ν_i,Hz)	0	470	940	1410	1880

- Simulation parameters

Parameter	**Value**
Carrier frequency (GHz)	4
Subcarrier spacing (kHz)	15
Frame size (M, N)	$(32, 32)$
Modulation scheme	BPSK

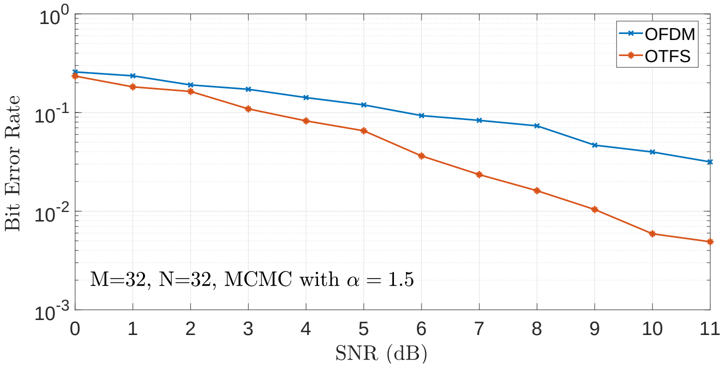

Figure: MCMC detector with temperature parameter $\alpha = 1.5$

PN-pilot based channel estimation for SISO-OTFS

- Consider the channel with P taps, $h(\tau,\nu) = \sum_{i=1}^{P} h_i \delta(\tau - \tau_i)\delta(\nu - \nu_i)$
- Coupling between input signal and the channel

$$\begin{aligned} y(t) &= \sum_{i=1}^{P} h_i x(t - \tau_i) e^{j2\pi\nu_i(t-\tau_i)} + v(t) \\ &= \sum_{i=1}^{P} h'_i e^{j2\pi\nu_i t} x(t - \tau_i) + v(t) \end{aligned}$$

where $h'_i = h_i e^{-j2\pi\nu_i\tau_i}$ and $v(t)$ is the AWGN noise

- Consider $\kappa_{\nu_i} = 0$ (no IDI)

$$y[k,l] = \sum_{i=1}^{P} h'_i x[((k - k_{\nu_i}))_N, ((l - l_{\tau_i}))_M)] + v[k,l]$$

- Vectorized form: $\mathbf{y} = \mathbf{H}\mathbf{x} + \mathbf{v}$

The discrete channel model

- Notations
  - $\mathcal{H}$: vector space of complex valued functions on the set of finite integers $\mathbb{Z}_{N_p} = \{0, 1, \cdots, N_p - 1\}$ equipped with addition and multiplication modulo N_p
  - Inner product in $\mathcal{H}$: $\langle f_1, f_2 \rangle = \sum_{n \in \mathbb{Z}_{N_p}} f_1[n]\overline{f_2[n]}$ and $e(t) = e^{\frac{j2\pi}{N_p}t}$
- Continuous time to discrete time conversion
  - Start with $S \in \mathcal{H}$ and let $S_A(t) = \sum_{n=0}^{M-1} S[n \bmod N_p]\mathrm{sinc}(Wt - n)$ where $M \geq N_p$
  - $T_{\text{spread}} = \max(\tau_i)$, $K \geq \lceil WT_{\text{spread}} \rceil$, $M = N_p + K$
  - Transmit $S_A(t)$ from time $t = 0$ to $t = \frac{M}{W}$
  - $R_A(t) = \sum_{i=1}^{P} h_i' e^{j2\pi\nu_i t} S_A(t - \tau_i) + v(t)$. Sample $R_A(t)$ at an interval $T_s = \frac{1}{W}$ from time $\frac{K}{W}$
  - $R[n] = R_A(\frac{(K+n)}{W})$, $n \in \mathbb{Z}_{N_p}$

- Discrete channel model

$$R[n] = \sum_{i=1}^{P} \alpha_i e(\omega_i n) S[n-\delta_i] + v[n], \;\; n \in \mathbb{Z}_{N_p}$$

$$\alpha_i = h_i' e^{(j2\pi\nu_i K/W)}, \;\; \delta_i = \tau_i W, \text{ and } \omega_i = N_p \nu_i / W, \;\; (\delta_i, \omega_i) \in \mathbb{Z}_{N_p}$$

- Channel estimation problem: Estimate $(\alpha_i, \delta_i, \omega_i)$ for $i = 1, 2, \cdots, P$
- Time-frequency shift (TFS) problem: estimate (δ_0, ω_0) given

$$R[n] = e(\omega_0 n) S[n-\delta_0] + v[n]$$

- Matched filter matrix of R and S

$$\mathcal{M}(R,S)[\delta,\omega] = \langle R[n], e(\omega n) S[n-\delta] \rangle, \;\; (\delta,\omega) \in \mathbb{Z}_{N_p} \times \mathbb{Z}_{N_p}$$

[1]

[1] A. Fish, S. Gurevich, R. Hadani, A. M. Sayeed, and O. Schwartz, "Delay-Doppler channel estimation in almost linear complexity," *IEEE Trans. Inf. Theory*, vol. 59, no. 11, pp. 7632-7644, Nov. 2013.

- Suppose $S \in \mathcal{H}$ is a PN sequence of norm one and $R,\ S$ satisfy $R[n] = e(\omega_0 n)S[n - \delta_0] + v[n]$
- As the length of the sequence N_p tends to infinity, with probability going to one

$$\begin{aligned} \mathcal{M}(R,S)[\delta,\omega] = &\ 1 + \epsilon'_{N_p} \ \ \textit{if}\ \ (\delta,\omega) = (\delta_0,\omega_0) \\ = &\ \epsilon_{N_p} \qquad\ \ \textit{if}\ \ (\delta,\omega) \neq (\delta_0,\omega_0) \end{aligned} \tag{3}$$

where $|\epsilon'_{N_p}| \leq \frac{1}{\sqrt{N_p}}$ and $|\epsilon_{N_p}| \leq \frac{(C+1)}{\sqrt{N_p}}$ for some constant $C > 0$

- Solution to TFS: Compute $\mathcal{M}(R,S)$ and choose (δ_0,ω_0) for which $\mathcal{M}(R,S)[\delta_0,\omega_0] \approx 1$
- Finally, (3) along with the bi-linearity of the inner product gives $\alpha_i \approx \mathcal{M}(R,S)[\delta_i,\omega_i],\ i = 1,2,\cdots,P$

Time-frequency shift problem

- SNR $= 0$ dB and $N_p = 127$

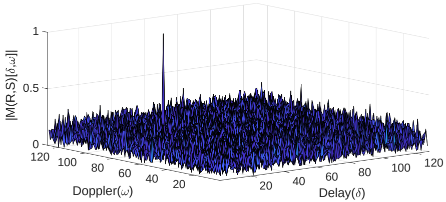

Figure: (δ_0, ω_0)=(40,90)

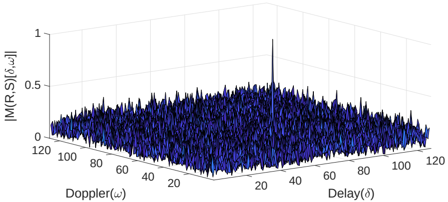

Figure: (δ_0, ω_0)=(80,60)

Channels with 2 delay-Doppler taps

- SNR = 20 dB, $\alpha_i \in \mathbb{C}$, and $N_p = 127$

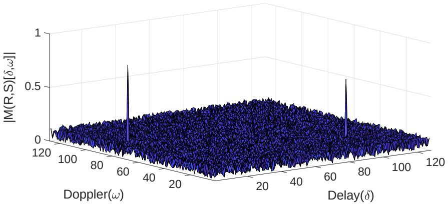

Figure: $(\delta_0, \omega_0, \delta_1, \omega_1)$=(100,30,10,80)

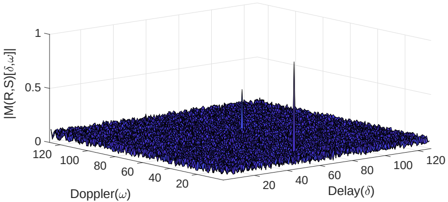

Figure: $(\delta_0, \omega_0, \delta_1, \omega_1)$=(60,20,70,70)

5 tap channel

- SNR $= 20$ dB, $(\delta_i, \omega_i) \in \{(10, 60), (20, 110), (30, 30), (80, 40), (110, 90)\}$

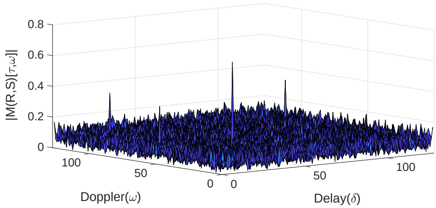

Figure: $N_p = 127$

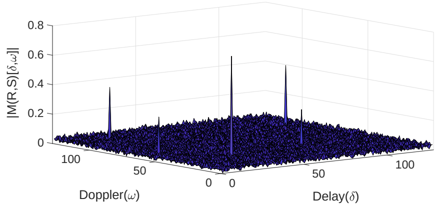

Figure: $N_p = 1023$

OTFS performance results with the estimated channel

- $\kappa_{\nu_i} = 0$ (no IDI) is assumed
- Delay and Doppler models

Path index (i)	1	2	3	4	5
Delay (τ_i,μs)	2.1	4.2	6.3	8.4	10.4
Doppler (ν_i,Hz)	0	470	940	1410	1880

- Simulation parameters

Parameter	**Value**
Carrier frequency (GHz)	4
Subcarrier spacing (kHz)	15
Frame size (M, N)	$(32, 32)$
Modulation scheme	BPSK

Estimation error

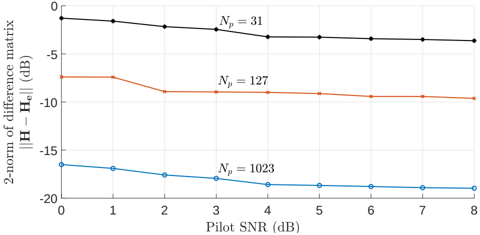

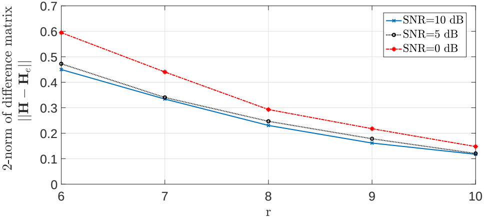

BER performance with the estimated channel

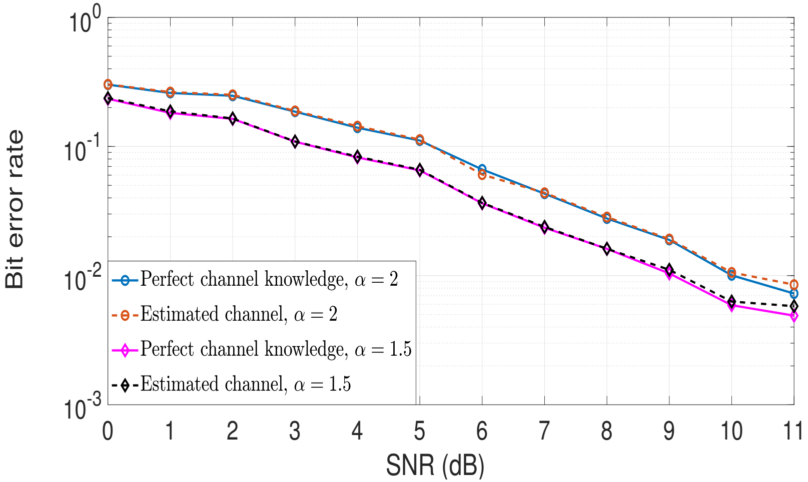

Figure: MCMC detector with temperature parameter α

- MCMC detection with $\alpha = 2$

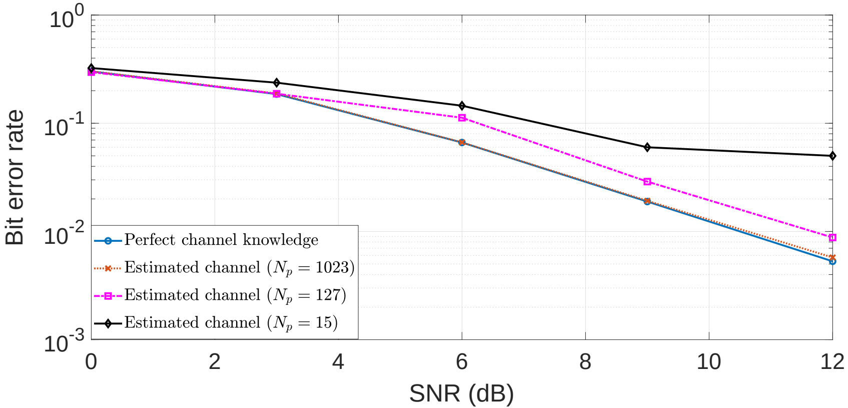

MIMO-OTFS modulation

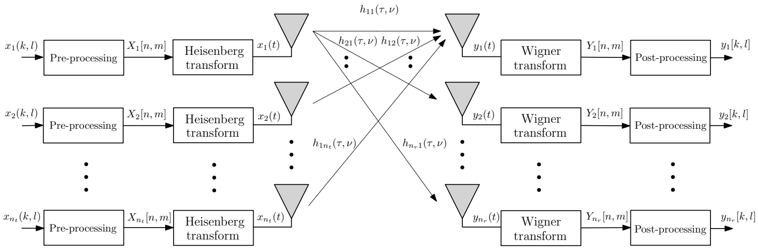

Figure: Block diagram of MIMO-OTFS modulation scheme

- n_t - number of transmit antennas, n_r - number of receive antennas
- Assume that the channel corresponding to pth transmit antenna and qth receive antenna is given by

$$h_{qp}(\tau,\nu) = \sum_{i=1}^{P} h_{qp_i}\delta(\tau-\tau_i)\delta(\nu-\nu_i),$$

$p = 1, 2, \cdots, n_t, \; q = 1, 2, \cdots, n_r$

Vectorized formulation of input-output relation

- Let the windows $W_{tx}[n, m]$, $W_{rx}[n, m]$ used for modulation be rectangular
- $\mathbf{H}_{qp}$ - equivalent channel matrix corresponding to pth transmit antenna and qth receive antenna
- $\mathbf{x}_p$ - $NM \times 1$ transmit vector from the pth transmit antenna in a given frame
- $\mathbf{y}_q$ - $NM \times 1$ received vector corresponding to qth receive antenna in a given frame
- Input-output relationship for the MIMO-OTFS system

$$
\begin{aligned}
\mathbf{y}_1 &= \mathbf{H}_{11}\mathbf{x}_1 + \mathbf{H}_{12}\mathbf{x}_2 + \cdots + \mathbf{H}_{1n_t}\mathbf{x}_{n_t} + \mathbf{v}_1 \\
\mathbf{y}_2 &= \mathbf{H}_{21}\mathbf{x}_1 + \mathbf{H}_{22}\mathbf{x}_2 + \cdots + \mathbf{H}_{2n_t}\mathbf{x}_{n_t} + \mathbf{v}_2 \\
&\vdots \\
\mathbf{y}_{n_r} &= \mathbf{H}_{n_r1}\mathbf{x}_1 + \mathbf{H}_{n_r2}\mathbf{x}_2 + \cdots + \mathbf{H}_{n_rn_t}\mathbf{x}_{n_t} + \mathbf{v}_{n_r}
\end{aligned}
$$

- Define

$$\mathbf{H}_{\text{MIMO}} = \begin{bmatrix} \mathbf{H}_{11} & \mathbf{H}_{12} & \dots & \mathbf{H}_{1n_t} \\ \mathbf{H}_{21} & \mathbf{H}_{22} & \dots & \mathbf{H}_{2n_t} \\ \vdots & \vdots & \ddots & \vdots \\ \mathbf{H}_{n_r1} & \mathbf{H}_{n_r2} & \dots & \mathbf{H}_{n_rn_t} \end{bmatrix},$$

$$\mathbf{x}_{\text{MIMO}} = [\mathbf{x}_1{}^T, \mathbf{x}_2{}^T, \cdots, \mathbf{x}_{n_t}{}^T]^T, \mathbf{y}_{\text{MIMO}} = [\mathbf{y}_1{}^T, \mathbf{y}_2{}^T, \cdots, \mathbf{y}_{n_r}{}^T]^T,$$
$$\mathbf{v}_{\text{MIMO}} = [\mathbf{v}_1{}^T, \mathbf{v}_2{}^T, \cdots, \mathbf{v}_{n_r}{}^T]^T.$$

- Linear system model, $\mathbf{y}_{\text{MIMO}} = \mathbf{H}_{\text{MIMO}}\mathbf{x}_{\text{MIMO}} + \mathbf{v}_{\text{MIMO}}$
- $\mathbf{x}_{\text{MIMO}} \in \mathbb{C}^{n_tNM\times 1}, \mathbf{y}_{\text{MIMO}}, \mathbf{v}_{\text{MIMO}} \in \mathbb{C}^{n_rNM\times 1}$, $\mathbf{H}_{\text{MIMO}} \in \mathbb{C}^{n_rNM\times n_tNM}$
- Only n_tP non-zero elements in each row and n_rP non-zero elements in each column of $\mathbf{H}_{\text{MIMO}}$

Vectorized formulation of input-output relation for MIMO-OFDM

- $\mathbf{H}_{\text{OFDM}_{qp}}$ - the equivalent channel matrix corresponding to pth transmit antenna and qth receive antenna
- $\mathbf{x}_{\text{OFDM}_p}$ - $NM \times 1$ transmit vector from the pth transmit antenna in a given frame
- $\mathbf{y}_{\text{OFDM}_q}$ denote the $NM \times 1$ received vector corresponding to qth receive antenna in a given frame
- Define

$$\mathbf{H}_{\text{MIMO-OFDM}} = \begin{bmatrix} \mathbf{H}_{\text{OFDM}_{11}} & \mathbf{H}_{\text{OFDM}_{12}} & \cdots & \mathbf{H}_{\text{OFDM}_{1n_t}} \\ \mathbf{H}_{\text{OFDM}_{21}} & \mathbf{H}_{\text{OFDM}_{22}} & \cdots & \mathbf{H}_{\text{OFDM}_{2n_t}} \\ \vdots & \vdots & \ddots & \vdots \\ \mathbf{H}_{\text{OFDM}_{n_r1}} & \mathbf{H}_{\text{OFDM}_{n_r2}} & \cdots & \mathbf{H}_{\text{OFDM}_{n_rn_t}} \end{bmatrix}$$

- Define

$$\mathbf{x}_{\text{MIMO-OFDM}} = [\mathbf{x}_{\text{OFDM}_1}{}^T, \mathbf{x}_{\text{OFDM}_2}{}^T, \cdots, \mathbf{x}_{\text{OFDM}_{n_t}}{}^T]^T,$$
$$\mathbf{y}_{\text{MIMO-OFDM}} = [\mathbf{y}_{\text{OFDM}_1}{}^T, \mathbf{y}_{\text{OFDM}_2}{}^T, \cdots, \mathbf{y}_{\text{OFDM}_{n_r}}{}^T]^T$$

- Linear system model, $\mathbf{y}_{\text{MIMO-OFDM}} = \mathbf{H}_{\text{MIMO-OFDM}}\mathbf{x}_{\text{MIMO-OFDM}} + \mathbf{v}_{\text{MIMO-OFDM}}$
- $\mathbf{x}_{\text{MIMO-OFDM}} \in \mathbb{C}^{n_t NM \times 1}, \mathbf{y}_{\text{MIMO-OFDM}}, \mathbf{v}_{\text{MIMO-OFDM}} \in \mathbb{C}^{n_r NM \times 1}$, $\mathbf{H}_{\text{MIMO-OFDM}} \in \mathbb{C}^{n_r NM \times n_t NM}$

Performance results

- $\kappa_{\nu_i} = 0$ (no IDI) is assumed
- Delay and Doppler models

Path index (i)	1	2	3	4	5
Delay (τ_i,μs)	2.1	4.2	6.3	8.4	10.4
Doppler (ν_i,Hz)	0	470	940	1410	1880

- Simulation parameters

Parameter	**Value**
Carrier frequency (GHz)	4
Subcarrier spacing (kHz)	15
Frame size (M, N)	$(32, 32)$
Modulation scheme	BPSK
MIMO configuration	1×1, 1×2, 1×3, 2×2, 3×3, 2×3
Maximum speed (kmph)	507.6

Table: System parameters.

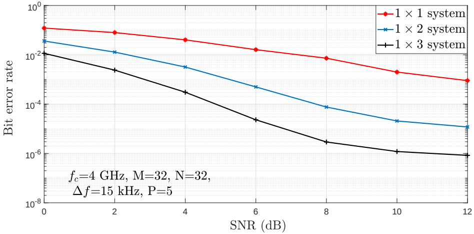

Figure: SISO, 1×2, 1×3

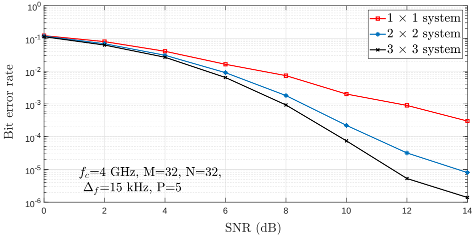

Figure: SISO, 2×2, 3×3

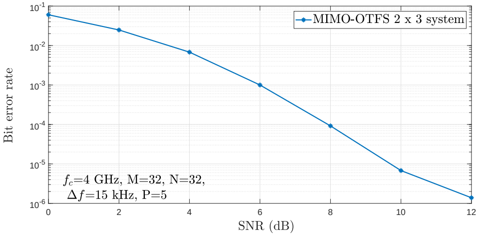

Figure: 2×3 system

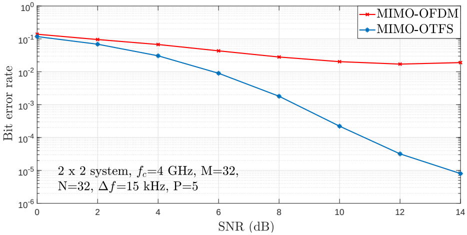

Figure: BER performance comparison between OTFS and OFDM

Channel estimation using impulses in the delay-Doppler domain

- Each transmit and receive antenna pair sees a different channel having a finite support in the delay-Doppler domain
- The support is determined by the delay and Doppler spread of the channel
- The OTFS input-output relation for pth transmit antenna and qth receive antenna pair can be written as

$$\hat{x}_q[k,l] = \sum_{m=0}^{M-1} \sum_{n=0}^{N-1} x_p[n,m] \frac{1}{MN} h_{w_{qp}}\left(\frac{k-n}{NT}, \frac{l-m}{M\Delta f}\right) + v_q[k,l].$$

- If we transmit

$$x_p[n,m] = 1 \text{ if } (n,m) = (n_p, m_p)$$
$$= 0 \ \forall \ (n,m) \neq (n_p, m_p),$$

as pilot from the pth antenna, the received signal at the qth antenna will be

$$\hat{x}_q[k,l] = \frac{1}{MN} h_{w_{qp}}\left(\frac{k-n_p}{NT}, \frac{l-m_p}{M\Delta f}\right) + v_q[k,l].$$

- $\frac{1}{MN} h_{w_{qp}}\left(\frac{k}{NT}, \frac{l}{M\Delta f}\right)$ and thus $\hat{\mathbf{H}}_{qp}$ can be estimated , since n_p and m_p are known at the receiver a priori
- Impulse at $(n,m) = (n_p, m_p)$ spreads only to the extent of the support of the channel in the delay-Doppler domain (2D convolution)
- If the pilot impulses have sufficient spacing in the delay-Doppler domain, they will be received without overlap

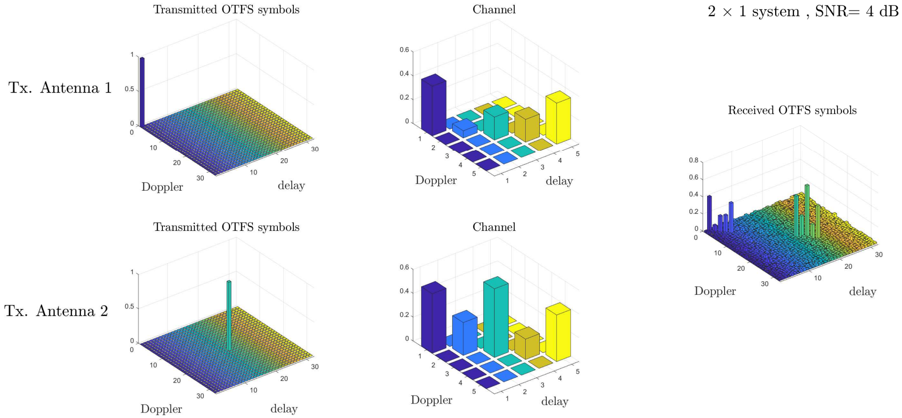

Figure: Illustration of pilots and channel response in delay-Doppler domain in a 2×1 MIMO-OTFS system

SISO OTFS system

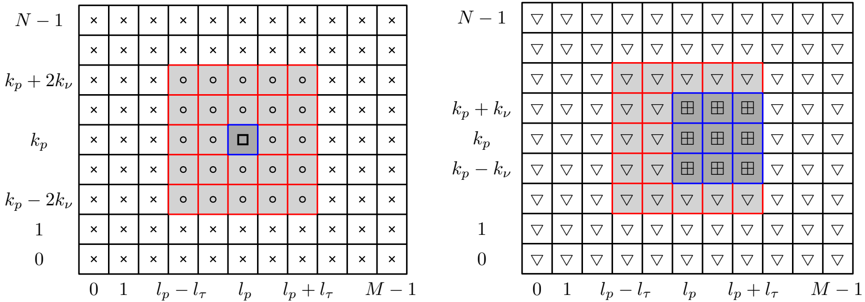

(a) Tx symbol arrangement (□: pilot; ∘: guard symbols; ×: data symbols)

(b) Rx symbol pattern (▽: data detection, ⊞: channel estimation)

Figure: Tx pilot, guard, and data symbols and Rx received symbols

SISO OTFS system with IDI

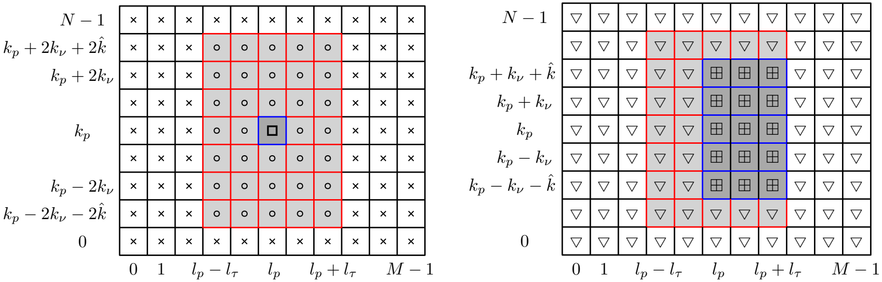

(a) Tx symbol arrangement (□: pilot; ∘: guard symbols; ×: data symbols)

(b) Rx symbol pattern (▽: data detection, ⊞: channel estimation)

Figure: Tx pilot, guard, and data symbols and Rx received symbols

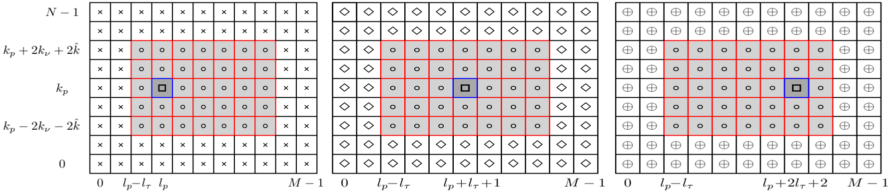

(a) Antenna 1 ($\times$: antenna 1 data symbol)

(b) Antenna 2 ($\Diamond$: antenna 2 data symbol)

(c) Antenna 3 ($\oplus$: antenna 3 data symbol)

Figure: Tx pilot, guard, and data symbols for MIMO OTFS system ($\Box$: pilot; $\circ$: guard)

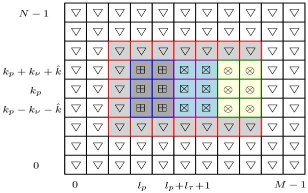

Figure: Rx symbol pattern at antenna 1 of MIMO OTFS system ($\triangledown$: data detection, $\boxplus, \boxtimes, \otimes$: channel estimation for Tx antenna 1, 2, and 3, respectively)

MIMO-OTFS performance with the estimated channel

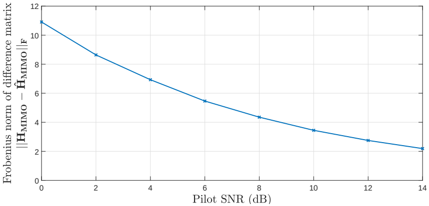

Figure: Frobenius norm of the difference matrix $\mathbf{H}_{\text{MIMO}} - \hat{\mathbf{H}}_{\text{MIMO}}$ as a function of pilot SNR in a 2×2 MIMO-OTFS system

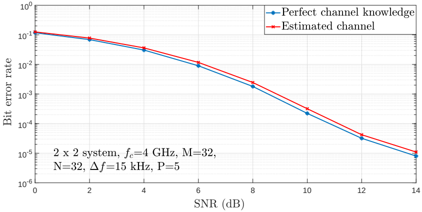

Figure: BER performance of 2×2 MIMO-OTFS system using the estimated channel

Multiuser OTFS system – uplink

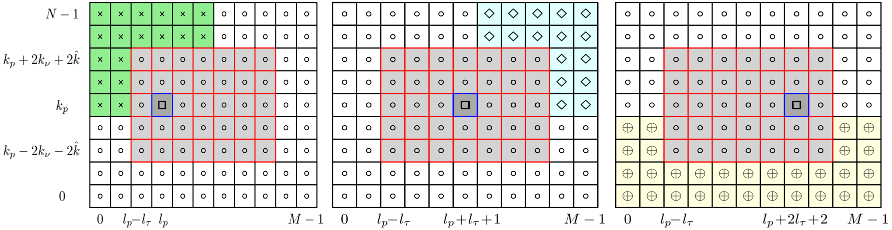

(a) User 1 ($\times$: user 1 data symbol)

(b) User 2 ($\Diamond$: user 2 data symbol)

(c) User 3 ($\oplus$: user 3 data symbol)

Figure: Tx pilot, guard, and data symbols for multiuser uplink OTFS system ($\square$: pilot; $\circ$: guard symbols)

Multiuser OTFS system – downlink

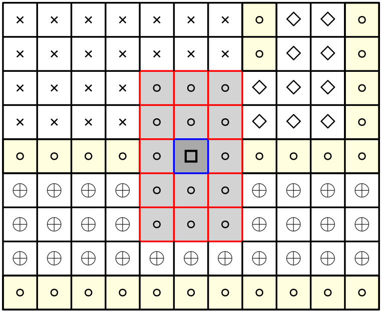

Figure: Tx pilot and data arrangement for multiuser downlink OTFS system ($\square$: pilot; $\circ$: guard symbols; $\times, \Diamond, \oplus$: data symbols for users 1, 2, and 3, respectively)

References I

1. R. Hadani, S. Rakib, M. Tsatsanis, A. Monk, A. J. Goldsmith, A. F. Molisch, and R. Calderbank, "Orthogonal time frequency space modulation," in *Proc. IEEE WCNC*, San Francisco, CA, USA, March 2017.
2. R. Hadani, S. Rakib, S. Kons, M. Tsatsanis, A. Monk, C. Ibars, J. Delfeld, Y. Hebron, A. J. Goldsmith, A.F. Molisch, and R. Calderbank, "Orthogonal time frequency space modulation," Available online: https://arxiv.org/pdf/1808.00519.pdf.
3. R. Hadani, and A. Monk, "OTFS: A new generation of modulation addressing the challenges of 5G," *OTFS Physics White Paper*, Cohere Technologies, 7 Feb. 2018. Available online: https://arxiv.org/pdf/1802.02623.pdf.
4. R. Hadani et al., "Orthogonal Time Frequency Space (OTFS) modulation for millimeter-wave communications systems," 2017 IEEE MTT-S International Microwave Symposium (IMS), Honolulu, HI, 2017, pp. 681-683.
5. A. Fish, S. Gurevich, R. Hadani, A. M. Sayeed, and O. Schwartz, "Delay-Doppler channel estimation in almost linear complexity," *IEEE Trans. Inf. Theory*, vol. 59, no. 11, pp. 7632–7644, Nov 2013.
6. A. Monk, R. Hadani, M. Tsatsanis, and S. Rakib, "OTFS - Orthogonal time frequency space: A novel modulation technique meeting 5G high mobility and massive MIMO challenges." Technical report. Available online: https://arxiv.org/ftp/arxiv/papers/1608/1608.02993.pdf.

References II

7. R. Hadani and S. Rakib. "OTFS methods of data channel characterization and uses thereof." U.S. Patent 9 444 514 B2, Sept. 13, 2016.
8. P. Raviteja, K. T. Phan, Q. Jin, Y. Hong, and E. Viterbo, "Low-complexity iterative detection for orthogonal time frequency space modulation," in *Proc. IEEE WCNC,* Barcelona, April 2018.
9. P. Raviteja, K. T. Phan, Y. Hong, and E. Viterbo, "Interference cancellation and iterative detection for orthogonal time frequency space modulation," *IEEE Trans. Wireless Commun.*, Available online: https://arxiv.org/abs/1802.05242.
10. P. Raviteja, K. T. Phan, Y. Hong, and E. Viterbo, "Embedded delay-Doppler channel estimation for orthogonal time frequency space modulation," *accepted in IEEE VTC2018-fall,* Chicago, USA, August 2018.
11. P. Raviteja, K. T. Phan, and Y. Hong, "Embedded delay-Doppler channel estimation based on pilot arrangement in OTFS systems," to be submitted in *IEEE Transactions on Vehicular Technology*.
12. Li Li, H. Wei, Y. Huang, Y. Yao, W. Ling, G. Chen, P. Li, and Y. Cai, "A simple two-stage equalizer With simplified orthogonal time frequency space modulation over rapidly time-varying channels," available online: https://arxiv.org/abs/1709.02505.
13. T. Zemen, M. Hofer, and D. Loeschenbrand, "Low-complexity equalization for orthogonal time and frequency signaling (OTFS)," available online: https://arxiv.org/pdf/1710.09916.pdf.

References III

14. Thomas Zemen, Markus Hofer, David Loeschenbrand, and Christoph Pacher, "Iterative detection for orthogonal precoding in doubly selective channels", available online: https://arxiv.org/pdf/1710.09912.pdf.
15. K. R. Murali, and A. Chockalingam, "On OTFS modulation for high-Doppler fading channels," in *Proc. ITA'2018,* San Diego, Feb. 2018.
16. M. K. Ramachandran, and A. Chockalingam, "MIMO-OTFS in high-Doppler fading channels: Signal detection and channel estimation," available online: https://arxiv.org/abs/1805.02209.
17. A. Farhang, A. RezazadehReyhani, L. E. Doyle and B. Farhang-Boroujeny, "Low complexity modem structure for OFDM-based orthogonal time frequency space modulation," in *IEEE Wireless Communications Letters,* vol. 7, no. 3, pp. 344-347, June 2018.
18. A. RezazadehReyhani, A. Farhang, M. Ji, R. R. Chen and B. Farhang-Boroujeny, "Analysis of discrete-time MIMO OFDM-based orthogonal time frequency space modulation," in *Proc. 2018 IEEE International Conference on Communications (ICC),* Kansas City, MO, USA, pp. 1-6, 2018.

Thank you!!